Transcriptional gene silencing by *Arabidopsis* microrchidia homologues involves the formation of heteromers

Guillaume Moissiard[a,1,2], Sylvain Bischof[a,2], Dylan Husmann[a], William A. Pastor[a], Christopher J. Hale[a], Linda Yen[a], Hume Stroud[a,3], Ashot Papikian[a], Ajay A. Vashisht[b], James A. Wohlschlegel[b], and Steven E. Jacobsen[a,c,4]

[a]Department of Molecular, Cell and Developmental Biology and [c]Howard Hughes Medical Institute, University of California, Los Angeles, CA 90095; and [b]Department of Biological Chemistry, David Geffen School of Medicine, University of California, Los Angeles, CA 90095

Contributed by Steven E. Jacobsen, April 14, 2014 (sent for review January 31, 2014)

Epigenetic gene silencing is of central importance to maintain genome integrity and is mediated by an elaborate interplay between DNA methylation, histone posttranslational modifications, and chromatin remodeling complexes. DNA methylation and repressive histone marks usually correlate with transcriptionally silent heterochromatin, however there are exceptions to this relationship. In *Arabidopsis*, mutation of *Morpheus Molecule 1* (*MOM1*) causes transcriptional derepression of heterochromatin independently of changes in DNA methylation. More recently, two *Arabidopsis* homologues of mouse microrchidia (MORC) genes have also been implicated in gene silencing and heterochromatin condensation without altering genome-wide DNA methylation patterns. In this study, we show that *Arabidopsis* microrchidia (AtMORC6) physically interacts with AtMORC1 and with its close homologue, AtMORC2, in two mutually exclusive protein complexes. RNA-sequencing analyses of high-order mutants indicate that *AtMORC1* and *AtMORC2* act redundantly to repress a common set of loci. We also examined genetic interactions between *AtMORC6* and *MOM1* pathways. Although *AtMORC6* and *MOM1* control the silencing of a very similar set of genomic loci, we observed synergistic transcriptional regulation in the *mom1*/*atmorc6* double mutant, suggesting that these epigenetic regulators act mainly by different silencing mechanisms.

epigenetics | plant biology

DNA methylation and histone posttranslational modifications are essential for silencing of transposable elements (TEs) and other repeat sequences. In the plant model organism *Arabidopsis thaliana*, DNA methylation sites are found in three different cytosine contexts: CG, CHG, and CHH (in which H is A, T, or C) (1). Symmetric CG and CHG methylations are mediated by DNA *Methyltransferase 1* (*MET1*) and *Chromomethylase 3* (*CMT3*), respectively (2, 3). Asymmetric CHH methylation is maintained at nonoverlapping sites by *CMT2* and *Domains Rearranged Methyltransferase 2* (*DRM2*) (4, 5). In the RNA-directed DNA methylation (RdDM) pathway, de novo methylation of CHH sites is established by *DRM2* and involves 24-nucleotide small interfering RNAs and long noncoding RNAs (6–11). Genome-wide studies revealed that DNA methylation and repressive histone modifications such as dimethylation of histone 3 lysine 9 (H3K9me2) correlate with transcriptionally silent chromatin (12–16). Furthermore, transcriptional derepression of silenced methylated loci is accompanied by loss of DNA methylation. A prominent exception to this interdependence is the *Morpheus Molecule 1* (*MOM1*).

MOM1 is unique to the plant kingdom and was identified in a random transfer-DNA (T-DNA) insertion screen reporting the derepression of a silenced transgene (17). The *mom1* mutant shows a loss of transcriptional gene silencing at loci located predominantly in the pericentromeric regions of the chromosomes (18). Interestingly, these transcriptional gene-silencing defects occur without major changes in DNA methylation or histone marks (17–21). *RNA Polymerase IV* and *V* (*PolIV* and *PolV*), which are key components of the RdDM pathway, were identified as enhancers of the *mom1* phenotype (18). To date, the extent to which *MOM1* is implicated in RdDM as well as its molecular mechanism of action remain poorly understood. Because *MOM1* shows partial sequence similarities to chromodomain–helicase–DNA binding proteins, it has been proposed that *MOM1* is involved in heterochromatin compaction (17, 22). However, the *mom1* mutant does not show any heterochromatin decondensation (20, 23).

Recently, members of the *Arabidopsis* microrchidia (AtMORC) ATPase family have also been shown to be involved in transposon repression and gene silencing (24–26). The *MORC1* gene was originally described in mice, where it was found to be essential for male primordial germ cell development (27, 28). The *Arabidopsis* genome contains seven *MORC* homologs, which were termed *AtMORC1* [NP_568000; AT4G36290; *Compromized Recognition of Turnip Crinkle Virus 1* (*CRT1*)], *AtMORC2* [NP_195351; AT4G36280; *CRT1–Homolog 1* (*CRH1*)], *AtMORC3* (NP_195350; AT4G36270; *CRH2*), *AtMORC4* (NP_199891; AT5G50780; *CRH4*), *AtMORC5* (NP_196817; AT5G13130; *CRH5*), *AtMORC6* [NP_173344; AT1G19100;

Significance

Members of the *Arabidopsis* microrchidia (AtMORC) ATPase family are involved in gene silencing and heterochromatin condensation without altering genome-wide DNA methylation patterns. Here, we examine the functional relationship between several family members and show that AtMORC6 interacts in two mutually exclusive protein complexes with AtMORC1 and its closest homologue, AtMORC2. Consistently, RNA sequencing of high-order mutants indicates that *AtMORC1* and *AtMORC2* act redundantly in gene silencing. We also examine the genetic interactions between *AtMORC6* and the transcriptional repressor *Morpheus Molecule 1* (*MOM1*). We observe a synergistic transcriptional regulation in the *mom1*/*atmorc6* double mutant, indicating that these epigenetic regulators act mainly in different silencing pathways, both independently of DNA methylation.

Author contributions: G.M., S.B., D.H., W.A.P., L.Y., A.P., and S.E.J. designed research; G.M., S.B., D.H., W.A.P., L.Y., and A.P. performed research; C.J.H., H.S., A.A.V., and J.A.W. analyzed data; and G.M., S.B., and S.E.J. wrote the paper.

The authors declare no conflict of interest.

Freely available online through the PNAS open access option.

Data deposition: The data reported in this paper have been deposited in the Gene Expression Omnibus (GEO) database, www.ncbi.nlm.nih.gov/geo (accession no. GSE54677).

[1]Present address: Department of Biology, ETH Zurich, 8092 Zurich, Switzerland.

[2]G.M. and S.B. contributed equally to this work.

[3]Present address: Department of Neurobiology, Harvard Medical School, Boston, MA 02115.

[4]To whom correspondence should be addressed. E-mail: jacobsen@ucla.edu.

This article contains supporting information online at www.pnas.org/lookup/suppl/doi:10.1073/pnas.1406611111/-/DCSupplemental.

www.pnas.org/cgi/doi/10.1073/pnas.1406611111

CRH6; *Defective in Meristem Silencing 11* (*DMS11*)], and *AtMORC7* (NP_194227; AT4G24970; *CRH3*) (25, 29–32). *AtMORC1* and *AtMORC2* are the most closely related homologs and share 80.9% amino acid sequence identity (29–32) (Fig. S1*A*). *AtMORC6* has been identified in four independent forward genetic screens (24–26, 31) as required for gene silencing and maintenance of heterochromatin integrity. *AtMORC1* is also required for gene silencing (26), although it was originally described as a master regulator in plant disease resistance signaling (30–33).

Currently, the molecular mechanisms by which the different *AtMORC* homologs achieve gene silencing remain to be elucidated. AtMORC proteins carry a gyrase, Hsp90, histidine kinase, and MutL (GHKL) domain together with an S5 domain that constitute an active adenosine triphosphatase (ATPase) module (27, 31, 34). They also carry a putative C-terminal coiled-coil domain (27). In vitro assays showed that both AtMORC1 and AtMORC6 are bona fide ATPases (26, 31). A modest reduction of DNA methylation and repressive histone marks at specific RdDM target sites in *atmorc6* mutant suggested that *AtMORC6* could also play a role in RdDM (24, 25). However, whole genome sequencing analyses of DNA methylation and H3K9me2 in *atmorc1* and *atmorc6* did not reveal significant differences compared with the wild-type level either in the genome at large or at sites of the highest level of gene derepression in *atmorc* mutants (26). Therefore, it is unlikely that the predominant function of AtMORC proteins is maintenance of DNA methylation and H3K9me2, although some interaction with the RdDM pathway seems likely.

In this study, we describe the physical interactions between three different AtMORC homologs and their functional implication in gene silencing. Biochemical analyses indicate that AtMORC6 forms mutually exclusive heteromers with AtMORC1 and its close homolog, AtMORC2. RNA-sequencing (RNA-seq) analyses of high-order mutants show that *AtMORC1* and *AtMORC2* act redundantly to repress a set of TEs similar to *AtMORC6*. Furthermore, we also examined the relationship between *AtMORC6*- and *MOM1*-mediated silencing as both pathways have only minor impacts on genome-wide DNA methylation. Interestingly, we observed a synergistic effect on transposon derepression, suggesting that these epigenetic regulators act by independent silencing mechanisms.

Results and Discussion

AtMORC6 Interacts in Vivo with AtMORC1 and AtMORC2 to Form Distinct Heteromers. Previous analyses showed similar transcriptional derepression between the single *atmorc6* single mutant and the *atmorc1*/*atmorc6* double mutant, suggesting that *AtMORC1* and *AtMORC6* could interact to enforce gene silencing (26). To test this hypothesis, FLAG epitope-tagged *AtMORC1* and *AtMORC6* under their respective endogenous promoters were introduced into *cmt3*/*atmorc1-3* and *atmorc6-1* lines, respectively. Western blotting analyses confirmed that both AtMORC1-FLAG and AtMORC6-FLAG were expressed in their respective mutant background and could complement the *suppressor of drm2 cmt3* (*SDC*)*::GFP* silencing defects (Fig. S1*B*). These lines were subsequently used to immunoprecipitate FLAG-tagged AtMORC proteins from leaf tissue, and mass spectrometry (MS) analyses were performed to determine potential interacting proteins. MS analyses indicated that AtMORC1 was strongly immunoprecipitated with AtMORC6-FLAG and vice versa (Table 1). This interaction was validated by coimmunoprecipitation (co-IP) using F_1 transgenic plant lines expressing complementing AtMORC1-myelocytomatosis (MYC) (26) and AtMORC6-FLAG (Fig. 1*A*).

To further characterize the interaction between AtMORC1 and AtMORC6, we performed gel filtration experiments. Leaf protein extracts from epitope-tagged lines were separated on a Superdex 200 10/300GL column, and the eluted fractions were probed by immunoblotting. We observed that both AtMORC1-FLAG and AtMORC6-FLAG were predominantly eluting around 200–300 KDa, suggesting that AtMORC proteins are primarily existing in vivo as dimers (Fig. S2). Together with the co-IP experiments, these results indicate that AtMORC1 and AtMORC6 are primarily found in vivo as heteromers, most likely as heterodimers. Nevertheless, it cannot be completely ruled out that AtMORC proteins might also form heterotetramers or higher molecular weight complexes, as we observed some signal in fractions with predicted sizes up to several hundred kilodaltons.

MS analysis of FLAG-tagged AtMORC6 IPs revealed an additional interaction with the closest homolog of AtMORC1, AtMORC2 (Table 1). This result is consistent with a recent independent study that also found peptides of AtMORC1 and AtMORC2 in an IP–MS of AtMORC6 in flowers (35). Interestingly, AtMORC2 was not immunoprecipitated with AtMORC1, suggesting that AtMORC6 was interacting with AtMORC1 and AtMORC2 in two distinct complexes (Table 1). To validate the heteromerization between AtMORC6 and AtMORC2, we engineered a complementing transgenic line expressing FLAG-tagged AtMORC2 in an *atmorc1*/*atmorc2* background (Fig. S1 *C* and *D*) and performed IP followed by MS. MS analysis showed that AtMORC6 was immunoprecipitated with FLAG-AtMORC2 (Table 1). Consistent with this interaction, gel filtration analysis of FLAG-AtMORC2 leaf extracts showed that

Table 1. FLAG-tagged AtMORC proteins were immunoprecipitated and interacting proteins were analyzed by MS

AtMORC6-FLAG IP

Name	Accession	Spectra		NSAF		% AtMORC6	
AtMORC6	AT1G19100	77	75	2,060	539	100	100
AtMORC1	AT4G36290	62	31	1,732	233	84	43
AtMORC2	AT4G36280	35	20	992	152	48	28

AtMORC1-FLAG IP

Name	Accession	Spectra		NSAF		% AtMORC1	
AtMORC1	AT4G36290	76	71	6,273	765	100	100
AtMORC6	AT1G19100	11	42	870	434	14	57

FLAG-AtMORC2 IP

Name	Accession	Spectra		NSAF		% AtMORC2	
AtMORC2	AT4G36280	65	—	370	—	100	—
AtMORC6	AT1G19100	32	—	172	—	47	—

The total numbers of identified spectra, the normalized spectral abundance factor (NSAF), and the percentage relative to the bait protein are given for two biological replicates.

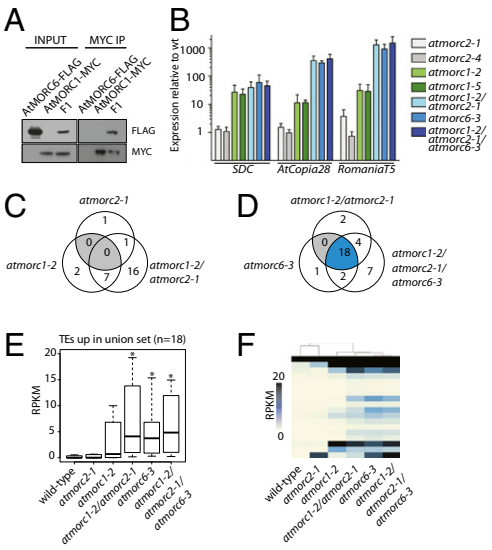

Fig. 1. Redundancy of *AtMORC1* and *AtMORC2* in transposon silencing. (*A*) AtMORC1 physically interacts with AtMORC6. AtMORC6-FLAG was coimmunoprecipitated with AtMORC1-MYC in F_1 plants expressing both epitope-tagged proteins. Epitope-tagged proteins were detected by Western blotting. (*B*) RT-PCR assessing endogenous expression of *SDC*, *AtCopia28*, and *RomaniaT5*. Three biological replicates were performed for each tested genotype. Two individual alleles were used for *atmorc1* and *atmorc2*. (*C* and *D*) Venn diagrams of overlap between TEs up-regulated (fourfold increase; FDR, 0.05; Fisher's exact test) in each genotype. Gray regions represent categories with no TEs counted. Blue shading represents the union set of TEs up-regulated in *atmorc* mutants. (*E*) Boxplot and (*F*) heatmap of average reads per kilo base per million (RPKM) values between two biological replicates for TEs in a union set for different genotypes. An asterisk indicates a significant increase relative to wild-type samples (P < 1e-3, Mann–Whitney U test).

FLAG-AtMORC2 was principally present in the elution fractions around 200–300 KDa, corresponding to similar elution fractions as AtMORC6-FLAG (Fig. S2). In summary, our biochemical analyses indicate that AtMORC6 physically interacts with AtMORC1 and AtMORC2 in the form of two mutually exclusive heteromers.

AtMORC6 was shown to interact in vitro with DMS3 when both proteins were coexpressed in *Escherichia coli*, providing a physical link to the RdDM pathway (25). DMS3 is a structural maintenance of chromosomes hinge domain-containing protein that lacks an ATPase domain (36). Based on the stimulation of AtMORC6 ATPase activity by in vitro interaction with DMS3, it was proposed that AtMORC6 and DMS3 cooperate to promote transcriptional repression. DMS3 has also been shown to interact with additional components of the DRD1-DMS3-RDM1 (DDR) complex including Defective in RNA-Directed DNA Methylation 1 (DRD1) or RDM1 as well as with the largest subunit of PolV (37). Furthermore, genome-wide association of PolV to chromatin and thus the production of PolV-dependent transcripts and subsequent DNA methylation are dependent on all members of the DDR complex (37, 38). However, we did not detect DMS3 or other components of the DDR complex in our IP–MS experiments. Also, previous IP–MS experiments using FLAG-tagged DRD1 and DMS3 proteins as bait did not immunoprecipitate AtMORC6 (37). Nevertheless, we cannot rule out that the interactions between components of the DDR complex and AtMORC6 are weak or ephemeral and could not be detected under our IP conditions.

A recent study found that AtMORC6 was immunoprecipitated in flowers in very small amounts with SUVH9, an SRA- (SET [suppressor of variegation 3–9 [Su(var)3–9], enhancer of zeste [E(z)], and trithorax (Trx)] and RING [really interesting new gene] associated)- and SET-domain-containing protein (35). SUVH9 and its closest homolog, SUVH2, were shown to bind methylated DNA and recruit PolV to chromatin through an interaction with the DDR complex (11, 35, 39). Yeast two-hybrid assays further indicated that the interactions between AtMORC proteins and SUVH proteins were direct (35). These data, together with the slight changes observed in DNA methylation of certain RdDM target loci (24, 25, 40), suggest that AtMORC proteins modulate RdDM through interactions with the DDR complex and SUVH proteins. Nevertheless, the mild changes of small RNAs and DNA methylation genome-wide in *atmorc* mutants (26) suggest that AtMORCs are unlikely to be canonical RdDM factors. It is also plausible that AtMORCs contribute to processing of target loci transcripts, thus leading to posttranslational silencing. Future experiments are needed to clarify the precise function in gene silencing and degree of involvement of AtMORCs in the RdDM pathway.

AtMORC2 Acts Redundantly with AtMORC1 to Achieve Gene Silencing. To further study the role of *AtMORC2* in gene silencing and its functional relationship with *AtMORC1* and *AtMORC6*, we generated high-order mutants and performed transcriptional profiling analyses. Real-time PCR (RT-PCR) from RNA extracted from leaf tissue indicated that *SDC* was derepressed in *atmorc1* but not *atmorc2* (Fig. 1*B*), consistent with the fact that *AtMORC2* was not identified in the genetic screens that identified *AtMORC1* and *AtMORC6* (24–26, 31). RT-PCR also showed an increased derepression of two transposons, *AtCopia28* and *RomaniaT5*, in the *atmorc1*/*atmorc2* double mutant compared with *atmorc1* and *atmorc2* single mutants (Fig. 1*B*), indicating that *AtMORC1* and *AtMORC2* act redundantly in transposon silencing. Further genome-wide characterization of the transcriptome by RNA-seq indicated that only two transposons was significantly up-regulated in *atmorc2* compared with wild type [using a very stringent cutoff of fold change ≥4; false discovery rate (FDR) < 0.05], whereas nine TEs were up-regulated in *atmorc1* (Fig. 1*C*). Transcriptional derepression of protein-coding genes was also more pronounced in *atmorc1* compared with *atmorc2* (Fig. 2*A*). Publicly available microarray data indicate that expression of *AtMORC1* is higher than *AtMORC2* in most tissues and developmental stages (Fig. S3*A*), providing a plausible explanation for the stronger silencing defects observed in *atmorc1* compared with *atmorc2*. Interestingly, combined deletion of *AtMORC1* and *AtMORC2* led to significantly higher transcription of TEs and protein-coding genes compared with both single mutants (Fig. 1 *C*, *E*, and *F* and Fig. 2 *A*, *C*, and *D*), confirming that *AtMORC1* and *AtMORC2* are functionally redundant. In addition, the overexpression of FLAG-AtMORC2 succeeded in complementing transcriptional derepression in the *atmorc1*/*atmorc2* double mutant (Fig. S1*D*).

The observed redundancy between *AtMORC1* and *AtMORC2* and their physical interaction with AtMORC6 in two mutually exclusive heteromers predict that a loss of *AtMORC6* should be phenotypically comparable to the combined loss of *AtMORC1* and *AtMORC2*. To test this hypothesis, we compared the transcriptomes of *atmorc1*/*atmorc2* with the *atmorc6* single mutant. RNA-seq revealed a high overlap of transcriptional derepression between *atmorc1*/*atmorc2* and *atmorc6* (Fig. 1 *D–F* and Fig. 2 *B–D*), supporting the notion that *AtMORC6* function is epistatic to both *AtMORC1* and *AtMORC2* combined. Derepressed transposons were not restricted to a specific family in any of the mutant backgrounds analyzed (Fig. S3*B*). Finally, the observed transcriptional derepression did not significantly increase in a triple mutant lacking *AtMORC1*, *AtMORC2*, and *AtMORC6* (Fig. 1 *D–F* and Fig. 2 *B–D*). These results are consistent with the model that AtMORC6 interacts exclusively with either AtMORC1 or AtMORC2 to achieve gene silencing and that *AtMORC1* is functionally redundant with *AtMORC2*.

It appeared that up-regulated genes were preferentially localized in H3K9me2-enriched heterochromatin (12) even though they are protein-coding (Fig. 2*E*). This is in agreement with the previous observations that *AtMORC1* and *AtMORC6* are mainly involved in silencing and compaction of heterochromatin (26). Gene ontology term analysis using AmiGO (41) of all up-regulated protein-coding genes indicated enrichments (P < 6e-4) in response

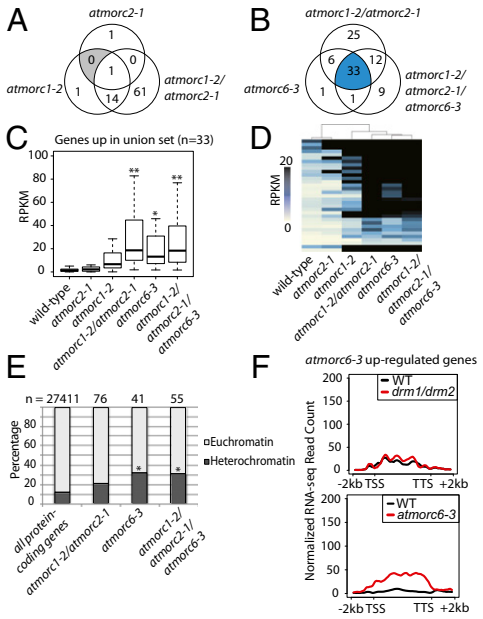

Fig. 2. Redundancy of *AtMORC1* and *AtMORC2* in gene silencing. (*A* and *B*) Venn diagrams showing relationships between sets of protein-coding genes called up-regulated (fourfold increase in expression; FDR < 0.05) for different genotypes. Gray regions represent categories with no gene counted. Blue shading represents the union set of genes up-regulated in *atmorc* mutants. (*C*) Boxplot and (*D*) heatmap of average RPKM values for different genotypes (two biological replicates) for protein-coding genes in a union set for different genotypes. An asterisk indicates a significant increase relative to wild-type samples (P < 1e-8, Mann–Whitney U test). Two asterisks represent a significant increase relative to wild-type samples and the *atmorc1* single mutant (P < 1e-2, Mann–Whintey U test). (*E*) Overrepresentation in H3K9me2-enriched heterochromatin of protein-coding genes significantly up-regulated in *atmorc1-2/atmorc2-1*, *atmorc6-3*, or *atmorc1-2/atmorc2-1/atmorc6-3* mutants. An asterisk indicates a significant increase relative to all protein-coding genes (P < 1e-3, Fisher's exact test). (*F*) Metagene analysis of RNA-seq reads over protein-coding genes called up-regulated in *atmorc1-2/atmorc2-1*, *atmorc6-3*, or *atmorc1-2/atmorc2-1/atmorc6-3* mutants. Reads are derived from previously published RNA-seq libraries for two replicates of the *drm1/drm2* double mutant and the corresponding wild type (WT).

to chitin and in response to organonitrogen compounds in *atmorc1/atmorc2* and in *atmorc1/atmorc2/atmorc6*. It is interesting to note that chitin has been recognized as a general elicitor of plant defense responses (42), which is in agreement with the reported implication of *AtMORC1* in plant immunity (31). To assess if protein-coding genes up-regulated in *atmorc6* were also targets of the RdDM machinery, we looked at their expression in a mutant lacking the methyltransferases *DRM1* and *DRM2* that is thus defective in RdDM (4). These were not significantly up-regulated in *drm1/drm2* (Fig. 2*F*), indicating that AtMORCs are unlikely to be canonical RdDM factors.

Our combined genetics and RNA-seq data show that the simultaneous absence of *AtMORC1* and *AtMORC2* in *atmorc1/atmorc2* cannot be functionally compensated by the presence of *AtMORC6* alone (Figs. 1 and 2). Also, the loss of *AtMORC6* in *atmorc6* cannot be compensated by the presence of *AtMORC1* and *AtMORC2* (Figs. 1 and 2). Furthermore, the *atmorc1/atmorc2/atmorc6* triple mutant does not have a stronger phenotype than the *atmorc1/atmorc2* double mutant (Fig. 1 *B* and *D–F* and Fig. 2 *B–D*). Together with the observation that AtMORC1 and AtMORC2 did not interact, these results lead to the conclusion that AtMORCs function as heteromers and not as homomers.

AtMORC6 and MOM1 Act Synergistically to Silence a Common Set of Transposons. *AtMORC1* and *AtMORC6* were identified in a forward genetic screen reporting the derepression of an *SDC::GFP* transgene in wild type or in the *cmt3* mutant background (26). Further screening of ethyl methanesulfonate (EMS) mutagenized seeds followed by deep genome resequencing identified two new alleles of *AtMORC6* in the *cmt3* background. In the first line, *cmt3* 262, glycine 212 was mutated to glutamic acid, and in *cmt3* 379, a guanine (chr1:6599258) was mutated to adenine in the splice site before exon 14. Interestingly, we also identified three loss-of-function alleles of the *MOM1* gene in the same genetic screen. The EMS mutations in these new *mom1* alleles were a stop codon introduced at amino acid 603 (line 337 in a wild-type background), a stop codon introduced at amino acid 586 (*cmt3* 265), and a substitution of Leucine 656 to Phenylalanine (*cmt3* 113).

MOM1 is unique to the plant kingdom and has no homologs in the *Arabidopsis* genome. Previous studies showed that DNA methylation in *mom1* mutants was similar to the wild-type level (17–19, 21). This observation was recently confirmed by genome-wide bisulfite-sequencing (BS-seq) analyses (43). RNA-seq analyses showed that 52 TEs were significantly up-regulated in *mom1* using similarly stringent cutoffs as for *atmorc* mutants (Fig. 3*A*), and we found that the DNA methylation levels of these TEs also remained unchanged in *mom1* compared with wild type (Fig. 3*D*). Nineteen transposons were significantly derepressed in *atmorc6* in this experiment, and most of these were also derepressed in *mom1* (Fig. 3*A*). The numbers of TEs significantly up-regulated in *atmorc6* slightly vary between the two RNA-seq experiments performed (Figs. 1*D* and 3*A*) because both experiments were done independently. As shown previously, DNA methylation was not significantly changed in TEs up-regulated in *atmorc6* (26) (Fig. 3*D*). These data indicate that overall transcriptional derepression is higher in *mom1* compared with *atmorc6* and that *MOM1* and *AtMORC6* mediate the silencing of a subset of common targets as well as of a number of independent loci.

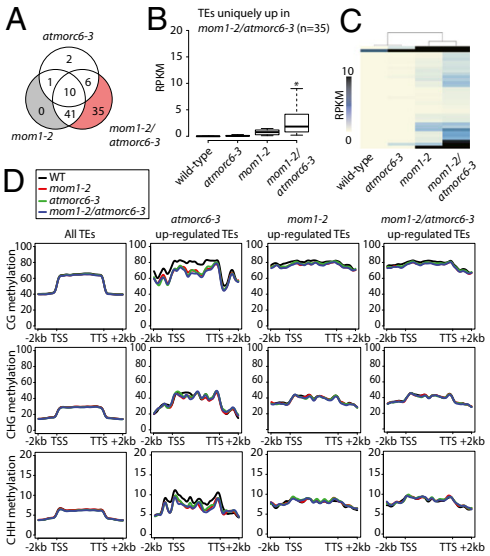

Fig. 3. Synergy of *AtMORC6* and *MOM1* in transposon silencing. (*A*) Venn diagram showing relationships between sets of TEs called up-regulated (fourfold increase in expression; FDR < 0.05) for different genotypes. Grayed regions highlight sets with no elements, and red shading highlights TEs uniquely called up-regulated in the higher order mutant. (*B*) Boxplot and (*C*) heatmap of average RPKM values between two biological replicates for TEs uniquely called up-regulated in the *mom1/atmorc6* mutant background for different genotypes. An asterisk indicates a significant increase relative to all other genotypes (P < 1e-8, Mann–Whitney U test). (*D*) Metagene analysis of DNA methylation levels across all *Arabidopsis* TEs for the *atmorc6-3*, *mom1-2*, *mom1-2/atmorc6-3*, and wild-type genotypes. Also shown are the methylation levels at TEs up-regulated in mutant genotypes.

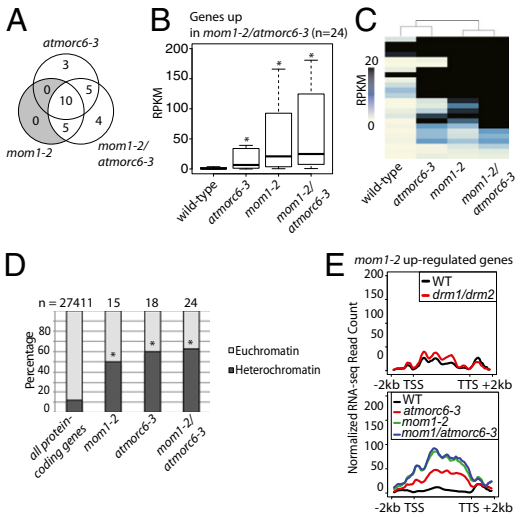

Fig. 4. Synergy of *AtMORC6* and *MOM1* in gene silencing. (*A*) Venn diagram showing relationships between sets of protein-coding genes called up-regulated (fourfold increase in expression; FDR < 0.05) for different genotypes. Grayed regions highlight sets with no elements. (*B*) Boxplot and (*C*) heatmap of average RPKM values for different genotypes (two biological replicates) for protein-coding genes uniquely called up-regulated in the *mom1/atmorc6* mutant background. An asterisk represents a significant increase relative to wild-type samples ($P < 1e\text{-}2$, Mann–Whitney *U* test). (*D*) Overrepresentation in H3K9me2-enriched heterochromatin of protein-coding genes significantly up-regulated in *atmorc6-3*, *mom1-2*, or *mom1-2/atmorc6-3* mutants. An asterisk indicates a significant increase relative to all protein-coding genes ($P < 1e\text{-}3$, Fisher's exact test). (*E*) Metagene analysis of RNA-seq reads over protein-coding genes called up-regulated in *atmorc6-3*, *mom1-2*, or *mom1-2/atmorc6-3* mutants. Reads are derived from previously published RNA-seq libraries for two replicates of the *drm1/drm2* double mutant and the corresponding wild type (WT).

To further understand the relationship between *MOM1*- and *AtMORC6*-mediated transcriptional silencing, we generated a double mutant lacking *MOM1* and *AtMORC6*. RNA-seq analyses in *mom1/atmorc6* showed a significant increase in derepression of TEs and to a smaller extent of protein-coding genes compared with both single mutants (Fig. 3 *A–C* and Fig. 4 *A–C*). RT-PCR analyses corroborated the synergistic derepression of *SDC* and *RomaniatT5* (Fig. S4*A*). Overexpressed TEs in all three genotypes profiled by RNA-seq are predominantly located in the pericentromeric heterochromatin and belong to diverse families, consistent with previous reports (18, 26) (Fig. S4 *B* and *C*). Genome-wide BS-seq analysis showed that DNA methylation was unchanged in TEs up-regulated in *mom1/atmorc6* (Fig. 3*D*). Similar to *AtMORC6* target loci, protein-coding genes significantly up-regulated in *mom1* were preferentially located in heterochromatin (Fig. 4*D*). Furthermore, transcription of these was not affected in the *drm1/drm2* mutant, suggesting a limited role of *MOM1* in RdDM (Fig. 4*E*). Altogether, these results indicate that *AtMORC6* and *MOM1* act synergistically to silence a largely common set of heterochromatic DNA elements through two independent pathways.

Conclusion

In this study, we combined biochemistry, genetics, and genomics to understand further the mode of action of the recently discovered *Arabidopsis* MORC homologs. We found that AtMORC6-mediated transcriptional silencing requires the formation of mutually exclusive heteromers with AtMORC1 and its closest homolog, AtMORC2. Further biochemical studies involving domain deletions or point mutations should uncover the molecular mechanisms of the AtMORC proteins and the implication of heteromerization for ATPase activity. It is interesting to note the similarities between AtMORCs and the structural maintenance of chromosome proteins cohesin and condensin (44). These three protein families are ATPases that function in vivo as heteromers and modulate chromatin superstructure to regulate proper expression and maintenance of genomic integrity.

Genetic and RNA-seq analyses showed that *AtMORC6* acts synergistically with the putative chromatin remodeler *MOM1* to silence a common set of heterochromatin-localized loci. The synergistic effect observed in the *mom1/atmorc6* double mutant suggests that *AtMORC6* and *MOM1* act in two convergent pathways that are both required for the proper silencing of pericentromeric heterochromatin. It has been previously shown that AtMORC6 and AtMORC1 accumulate in the nucleus as discrete nuclear bodies that localize in the vicinity of the heterochromatic chromocenters (26). It will be interesting to determine in the future whether MOM1 accumulates in a similar fashion in the nucleus to form distinct nuclear bodies. The identification of MOM1 interactors will also be crucial to understanding its mode of action.

Materials and Methods

Plant Material and Growing Conditions. Wild-type and all mutant lines are from the ecotype Columbia and were grown under continuous light. Plant lines used include *atmorc1-2* (SAIL_893_B06; crt1-2), *atmorc1-4* (SAIL_1239_C08), *atmorc1-5* (SAIL_131_H11; crt1-5), *atmorc2-1* (SALK_072774C; crh1-1), *atmorc2-4* (SALK_021267C; crh1-4), *atmorc6-3* (GABI_599B06), *cmt3-11* (SALK_148381), and *mom1-2* (SAIL_610_G01). EMS mutagenized *atmorc6-1* and *cmt3/morc1-3* lines and complementing AtMORC1-MYC and AtMORC6-MYC lines are described in ref. 26. T-DNA insertions were confirmed by PCR-based genotyping. Primer sequences are described in Table S1.

Cloning of pAtMORC1::AtMORC1-FLAG, pAtMORC2::FLAG-AtMORC2, and pAtMORC16::AtMORC6-FLAG. Cloning was done according to ref. 26. Briefly, AtMORC1 and AtMORC6 genomic regions were PCR amplified and the FLAG epitope was added to the C terminus of AtMORC1 and AtMORC6 and at the N terminus of AtMORC2. The amplified region includes a ~1 Kb promoter sequence upstream of the respective transcriptional start site.

IP and MS Analysis. Ten grams of 2-wk-old seedling tissue of each epitope-tagged line were ground in liquid nitrogen and resuspended in 45 mL ice-cold IP buffer [50 mM Tris·HCl pH 8.0, 150 mM NaCl, 5 mM $MgCl_2$, 0.1% Nonidet P-40, 10% (vol/vol) glycerol, 1× Protease Inhibitor Mixture (Roche)] and centrifuged for 10 min at 4 °C at 16,000 × *g*. We added 200 μL M2 magnetic FLAG-beads (SIGMA, M8823) to the supernatants and incubated it for 60 min rotating at 4 °C. M2 magnetic FLAG-beads were washed five times in ice-cold IP buffer for 5 min rotating at 4 °C, and immunoprecipitated proteins were eluted three times with 100 μL 3×-FLAG peptides (SIGMA, F4799) for 15 min at 25 °C. The eluted protein complexes were precipitated by trichloroacetic acid and subjected to MS analyses as previously described (14).

Co-IP and Immunoblotting. We ground 1.5 g of 2-wk-old seedling tissue of each epitope-tagged line in liquid nitrogen, resuspended it in 12 mL ice-cold IP buffer [50 mM Tris·HCl pH 8.0, 150 mM NaCl, 5 mM $MgCl_2$, 0.1% Nonidet P-40, 10% (vol/vol) glycerol, 1× Protease Inhibitor Mixture (Roche)], and centrifuged it for 10 min at 4 °C at 16,000 × *g*. We added 100 μL M2 magnetic FLAG-beads (SIGMA, M8823) or 150 μL MYC-conjugated agarose beads (COVANCE, AFC-150P-1000) to the supernatants and incubated it for 60 min rotating at 4 °C. Beads were washed five times in ice-cold IP buffer for 5 min rotating at 4 °C, and immunoprecipitated proteins were eluted in 1× Lämmli buffer for 15 min at 80 °C.

Western blots were performed as previously described (26) with GFP-specific antibody (Invitrogen, AA1122), HRP-coupled FLAG-specific antibody (SIGMA, A8592), and MYC-specific antibody (Pierce, MA1-980).

Gel Filtration. Gel filtration experiments were performed according to ref. 37. Briefly, 0.5 g of 2-wk-old seedling tissue of each epitope-tagged line were ground in liquid nitrogen and resuspended in 1 mL of ice-cold IP buffer [50 mM Tris·HCl pH 8.0, 150 mM NaCl, 0.1% Nonidet P-40, 10% (vol/vol) glycerol, 1× Protease Inhibitor Mixture (Roche)] and centrifuged for 10 min at 4 °C at 16,000 × *g*. The supernatants were centrifuged again for 10 min at 4 °C at 16,000 × *g*. The supernatants were then centrifuged through a 0.2 μm filter (Millipore), 500 μL were loaded onto a Superdex 200 10/300GL column (GE Healthcare, 17–5175-01) column, and 250 μL fractions were collected. We ran 20 μL of every collected fraction on a 4–12% SDS/PAGE. Before use, the column was equilibrated and calibrated with gel filtration standards (Biorad, 151–1901).

RNA Extraction. We froze 100 mg of 20-d-old leaf tissue in liquid nitrogen. The frozen leaves were then added to a mortar containing liquid nitrogen. Immediately after the liquid nitrogen boiled off, the leaf tissue was crushed to powder using a pestle. We immediately added 1.2 mL of TRIzol Reagent (Life Technologies 15596) to the cold powder, and then it was pulverized further until a clear, dark brown solution was visible. The solution was transferred to a chilled Eppendorf tube, and 400 μL of chloroform was added. The tube was vortexed for 5 s at maximum power, then spun in a centrifuge at 16,000 × *g* (4 °C) for 10 min to separate the aqueous and organic phases. We collected 700 μL of the aqueous (top) phase. To precipitate the RNA, 700 μL of isopropanol was added to the aqueous material, the solution was vortexed for 5 s at maximum power, and then it was centrifuged for 10 min at 16,000 × *g* (4 °C). The supernatant was removed, and 500 μL of room temperature 80% (vol/vol) ethanol was added to the pellet, which was then spun for 5 min at 16,000 × *g* (4 °C). The supernatant was removed and the pellet was air-dried for 5 to 10 min. The pelleted RNA was resuspended in 100 μL water and then purified using the Qiagen RNeasy Mini (Qiagen 74104) "RNA Cleanup Protocol" according to manufacturer's instructions. RNA was quantified using Nanodrop.

RT-PCR. We treated 1 μg of input RNA with DNase I (Life Technologies, 18068) according to the manufacturer's protocol. Of the 11 μL final reaction volume, 3 μL was set aside as a negative control for RT-PCR, whereas 8 μL was converted to cDNA using SuperScript III (Life Technologies 18080). We used 5% of cDNA for each RT-PCR. RT-PCR was performed using IQ SYBR Green Supermix (Bio-Rad 170–8880), with 375 nM final primer concentration using a Stratagene Mx3005p instrument. Amplification conditions were as follows: 95 °C 10:00; 40 cycles, 95 °C, 30 s, 55 °C 1:00, 72 °C 1:00; melting curve. At least two technical replicates were performed per biological replicate, and three biological replicates were used in all experiments. Relative abundance of transcripts was calculated using the difference of squares method. Primer sequences are described in Table S1.

BS-Seq, RNA-Seq, and Accession Codes. BS-seq was done according to ref. 26. RNA-seq libraries were generated using 2 μg of input RNA using TruSeq RNA Sample Preparation Kit v2 (Illumina RS-122-2001) according to the manufacturer's protocols. Sequencing data were deposited into Gene Expression Omnibus under accession no. GSE54677.

ACKNOWLEDGMENTS. We are grateful to Daniel F. Klessig (Boyce Thompson Institute for Plant Research, Ithaca, NY) for the *atmorc1/atmorc2* double knockout line. We are grateful to Michael F. Carey for his advice and for providing access to equipment. High-throughput sequencing was performed in the University of California, Los Angeles (UCLA) Broad Stem Cell Research Center BioSequencing Core Facility, and we are especially grateful to Mahnaz Akhavan for her support. We thank Bhumika Parekh, Colin Shew, Beatrice Sun, Lillian Tao, and Vanessa Trieu for technical assistance. This work was supported by National Institutes of Health (NIH) Grant GM60398 (to S.E.J.). C.J.H. is supported by the Damon Runyon postdoctoral fellowship, W.A.P. is supported by the Jane Coffin Childs Memorial Fund for Medical Research, H.S. is supported by a UCLA Dissertation Year Fellowship, L.Y. is supported by Ruth L. Kirschstein National Research Service Award GM007185, S.B. is supported by a postdoctoral fellowship of the Swiss National Science Foundation, and J.A.W. is supported by NIH Grant GM089778. S.E.J. is an investigator of the Howard Hughes Medical Institute.

1. Law JA, Jacobsen SE (2010) Establishing, maintaining and modifying DNA methylation patterns in plants and animals. *Nat Rev Genet* 11(3):204–220.
2. Jackson JP, Lindroth AM, Cao X, Jacobsen SE (2002) Control of CpNpG DNA methylation by the KRYPTONITE histone H3 methyltransferase. *Nature* 416(6880):556–560.
3. Ronemus MJ, Galbiati M, Ticknor C, Chen J, Dellaporta SL (1996) Demethylation-induced developmental pleiotropy in Arabidopsis. *Science* 273(5275):654–657.
4. Stroud H, et al. (2014) Non-CG methylation patterns shape the epigenetic landscape in Arabidopsis. *Nat Struct Mol Biol* 21(1):64–72.
5. Zemach A, et al. (2013) The Arabidopsis nucleosome remodeler DDM1 allows DNA methyltransferases to access H1-containing heterochromatin. *Cell* 153(1):193–205.
6. Cao X, Jacobsen SE (2002) Role of the arabidopsis DRM methyltransferases in de novo DNA methylation and gene silencing. *Curr Biol* 12(13):1138–1144.
7. Chan SW, et al. (2004) RNA silencing genes control de novo DNA methylation. *Science* 303(5662):1336.
8. Herr AJ, Jensen MB, Dalmay T, Baulcombe DC (2005) RNA polymerase IV directs silencing of endogenous DNA. *Science* 308(5718):118–120.
9. Law JA, et al. (2013) Polymerase IV occupancy at RNA-directed DNA methylation sites requires SHH1. *Nature* 498(7454):385–389.
10. Onodera Y, et al. (2005) Plant nuclear RNA polymerase IV mediates siRNA and DNA methylation-dependent heterochromatin formation. *Cell* 120(5):613–622.
11. Johnson LM, et al. (2014) SRA- and SET-domain-containing proteins link RNA polymerase V occupancy to DNA methylation. *Nature* 507(7490):124–128.
12. Bernatavichute YV, Zhang X, Cokus S, Pellegrini M, Jacobsen SE (2008) Genome-wide association of histone H3 lysine nine methylation with CHG DNA methylation in Arabidopsis thaliana. *PLoS ONE* 3(9):e3156.
13. Cokus SJ, et al. (2008) Shotgun bisulphite sequencing of the Arabidopsis genome reveals DNA methylation patterning. *Nature* 452(7184):215–219.
14. Du J, et al. (2012) Dual binding of chromomethylase domains to H3K9me2-containing nucleosomes directs DNA methylation in plants. *Cell* 151(1):167–180.
15. Johnson L, Cao X, Jacobsen S (2002) Interplay between two epigenetic marks. DNA methylation and histone H3 lysine 9 methylation. *Curr Biol* 12(16):1360–1367.
16. Tariq M, et al. (2003) Erasure of CpG methylation in Arabidopsis alters patterns of histone H3 methylation in heterochromatin. *Proc Natl Acad Sci USA* 100(15):8823–8827.
17. Amedeo P, Habu Y, Afsar K, Mittelsten Scheid O, Paszkowski J (2000) Disruption of the plant gene MOM releases transcriptional silencing of methylated genes. *Nature* 405(6783):203–206.
18. Yokthongwattana C, et al. (2010) MOM1 and Pol-IV/V interactions regulate the intensity and specificity of transcriptional gene silencing. *EMBO Journal* 29:340–351.
19. Habu Y, et al. (2006) Epigenetic regulation of transcription in intermediate heterochromatin. *EMBO Rep* 7(12):1279–1284.
20. Probst AV, Fransz PF, Paszkowski J, Mittelsten Scheid O (2003) Two means of transcriptional reactivation within heterochromatin. *Plant J* 33(4):743–749.
21. Vaillant I, Schubert I, Tourmente S, Mathieu O (2006) MOM1 mediates DNA-methylation-independent silencing of repetitive sequences in Arabidopsis. *EMBO Rep* 7(12):1273–1278.
22. Caikovski M, et al. (2008) Divergent evolution of CHD3 proteins resulted in MOM1 refining epigenetic control in vascular plants. *PLoS Genet* 4(8):e1000165.
23. Mittelsten Scheid O, Probst AV, Afsar K, Paszkowski J (2002) Two regulatory levels of transcriptional gene silencing in Arabidopsis. *Proc Natl Acad Sci USA* 99(21):13659–13662.
24. Brabbs TR, et al. (2013) The stochastic silencing phenotype of Arabidopsis morc6 mutants reveals a role in efficient RNA-directed DNA methylation. *Plant J* 75(5):836–846.
25. Lorković ZJ, Naumann U, Matzke AJ, Matzke M (2012) Involvement of a GHKL ATPase in RNA-directed DNA methylation in Arabidopsis thaliana. *Curr Biol* 22(10):933–938.
26. Moissiard G, et al. (2012) MORC family ATPases required for heterochromatin condensation and gene silencing. *Science* 336(6087):1448–1451.
27. Inoue N, et al. (1999) New gene family defined by MORC, a nuclear protein required for mouse spermatogenesis. *Hum Mol Genet* 8(7):1201–1207.
28. Watson ML, et al. (1998) Identification of morc (microrchidia), a mutation that results in arrest of spermatogenesis at an early meiotic stage in the mouse. *Proc Natl Acad Sci USA* 95(24):14361–14366.
29. Langen G, et al. (2014) The compromised recognition of turnip crinkle virus1 subfamily of microrchidia ATPases regulates disease resistance in barley to biotrophic and necrotrophic pathogens. *Plant Physiol* 164(2):866–878.
30. Kang HG, Klessig DF (2008) The involvement of the Arabidopsis CRT1 ATPase family in disease resistance protein-mediated signaling. *Plant Signal Behav* 3(9):689–690.
31. Kang HG, Kuhl JC, Kachroo P, Klessig DF (2008) CRT1, an Arabidopsis ATPase that interacts with diverse resistance proteins and modulates disease resistance to turnip crinkle virus. *Cell Host Microbe* 3(1):48–57.
32. Kang HG, et al. (2010) Endosome-associated CRT1 functions early in resistance gene-mediated defense signaling in Arabidopsis and tobacco. *Plant Cell* 22(3):918–936.
33. Kang HG, et al. (2012) CRT1 is a nuclear-translocated MORC endonuclease that participates in multiple levels of plant immunity. *Nat Commun* 3:1297.
34. Dutta R, Inouye M (2000) GHKL, an emergent ATPase/kinase superfamily. *Trends Biochem Sci* 25(1):24–28.
35. Liu ZW, et al. (2014) The SET domain proteins SUVH2 and SUVH9 are required for Pol V occupancy at RNA-directed DNA methylation loci. *PLoS Genet* 10(1):e1003948.
36. Kanno T, et al. (2008) A structural-maintenance-of-chromosomes hinge domain-containing protein is required for RNA-directed DNA methylation. *Nat Genet* 40(5):670–675.
37. Law JA, et al. (2010) A protein complex required for polymerase V transcripts and RNA-directed DNA methylation in Arabidopsis. *Curr Biol* 20(10):951–956.
38. Zhong X, et al. (2012) DDR complex facilitates global association of RNA polymerase V to promoters and evolutionarily young transposons. *Nat Struct Mol Biol* 19(9):870–875.
39. Johnson LM, Law JA, Khattar A, Henderson IR, Jacobsen SE (2008) SRA-domain proteins required for DRM2-mediated de novo DNA methylation. *PLoS Genet* 4(11):e1000280.
40. Lorković ZJ (2012) MORC proteins and epigenetic regulation. *Plant Signal Behav* 7(12):1561–1565.
41. Carbon S, et al.; AmiGO Hub; Web Presence Working Group (2009) AmiGO: Online access to ontology and annotation data. *Bioinformatics* 25(2):288–289.
42. Boller T (1995) Chemoperception of microbial signals in plant-cells. *Annu Rev Plant Physiol* 46:189–214.
43. Stroud H, Greenberg MV, Feng S, Bernatavichute YV, Jacobsen SE (2013) Comprehensive analysis of silencing mutants reveals complex regulation of the Arabidopsis methylome. *Cell* 152(1-2):352–364.
44. Wood AJ, Severson AF, Meyer BJ (2010) Condensin and cohesin complexity: The expanding repertoire of functions. *Nat Rev Genet* 11(6):391–404.